Turbine Design Technical Report

for the

Department of Energy
Collegiate Wind Competition

University of Maryland, College Park

Academic Advisors: Dr. James Baeder and Dr. VT Nagaraj (Aerospace Engineering)
3179 Glenn L. Martin Hall
College Park, Maryland, 20742
Phone: 301-405-1107; Fax: 301-314-9001
Email: baeder@umd.edu
Graduate Advisors: Brent Mills, Robert Brown
Team Lead:
Shelli Bond (Mechanical Engineering)
Aerodynamics:
Faisal Al Otaibi (Aerospace Engineering)
Brandon Tsou (Aerospace Engineering)
Tower Design:
Seva Zhuravskiy (Mechanical Engineering)
Electronics Generator:
Andrew Nixon (Electrical Engineering)
Anders Alilio (Mechanical Engineering)
Ian Decker (Mechanical Engineering)
Controls:
Pat Fox (Aerospace Engineering)
Structures:
Matt Johnson (Mechanical Engineering)

May 28th, 2020

Contents

1 Executive Summary

The University of Maryland, College Park Wind TERPines club submits this technical document to the Department of Energy Collegiate Wind Competition (CWC) as a detailed description of a small-scale wind turbine. It was not possible to fully meet the original goal of building a wind turbine because of the global health crisis. Recognizing these problems, the DOE modified the rules of the competition. Without direct access to labs, supplies and teammates, physical progress and data collection became impossible after the University of Maryland, along with nearly every school in the nation, shut its doors in March. However, enthusiasm for the project was not lost, and the goal of building a turbine through whatever means necessary remained real for each member, even if that meant designing one with CAD software or working in a makeshift home lab. This Report will show that despite these handicaps, we have been able to fulfil all the requirements of the DOE.

Table 1 is a summary of the new features of this design. First, the aerodynamics of the rotor blades and turbine-housing are discussed. Emphasis is placed on the rationale for airfoil selection and adherence to CWC rules. Next, focus shifts to the generator and what progress was made in optimizing it to capture the maximum amount of energy from wind. This is followed by an overview of the electrical system, featuring a system-wide one-line diagram and a plan for the emergency cut-off switch. The document concludes with an in-depth outline of the control system, which ensures that the turbine not only follows all guidelines, but also delivers appropriate power to the Point of Common Coupling (PCC) and the load. Unfortunately, it was not possible to build and test the turbine, but the design was carefully planned. An additional benefit of these unique social circumstances is that this year's design work will aid next year's UMD CWC team.

Table 1: *List format of all notable features*

	Significant Features	**Description**
Aero	Carbon fiber rotor blades	Lightweight blades for low rotor disk inertia.
	Pitch mechanism	Variable blade pitch used to control power and rotor speed above rated wind speed. Also used to maximize torque below cut-in speed.
Control	Closed-loop control design	Closed loop control actively monitors outputs and adjusts to seek optimal power coefficients. More robust than open loop control.
	Kalman filter sensor fusion	Combines sensor data to infer tip speed ratio during below rated speed operation.
	Pitot tubes	Direct measurement of wind speed allows for accurate closed-loop control.
	Variable buck-boost converter	Variable load is simulated by modulating voltage at the PCC. This also allows for control of rotor RPM using motor torque.
Generation	Load power supply	Turbine control, sensors, and actuators are active even when power is not generated. They are powered through the load, drawing power from the 'grid'.
	Manually wound generator	Generator is modified by re-wrapping windings to achieve a super-low kV value, which allows for power generation at relatively low RPMs.
Yaw	Grid fin	The grid fin is a honeycomb structure with an extremely high surface area, which allows for responsive yaw rates even at low wind speeds.
Braking	Ratcheting one-way pitch bearing	One-way bearing used for braking turbine while causing minimal stress on actuators and blades. Blades are yawed to a negative angle of attack, and bearing does not rotate in the opposite direction.
	MOSFET power bleed transistor	Field effect transistor used to convert excess power to heat for effective braking in high winds.

2 Design Iteration

As the shift of this year's design project moved into the digital world, the UMD Wind Terpines had only a slight shift in our design objective. Perhaps we were no longer able to build our turbine, but we were still motivated to think through all of the challenges we would have seen if we ever had the chance to test our turbine for its ability to cut in at low speeds, maximize its power curve, maintain control for rated power and rotor speed, cut out on-demand for safety, withstand high winds from rapidly changing directions, and shift into a park mode when the wind speed exceeds 22 m/s. Nearly a dozen designs were considered, but after first completing a Pugh Matrix, the configuration was narrowed to four options.

1. A three-bladed, pitch and torque controlled horizontal axis wind turbine.
2. A ducted wind turbine with fixed pitch that accelerates airflow to more than twice the freestream velocity, extracting maximum power.
3. An Archimedes screw, which would allow for high power coefficient at low wind speed.
4. A small Archimedes screw with airfoil-style fixed-pitch blades around the outer radius of the Archimedes screw, striking a balance between low and high wind speed performance.

Next, the team used the Analytic Hierarchy Process (AHP) to select our final design configuration. This process compares design architectures against each other across a series of weighted design considerations. Table 2 shows the first step in this process. Ultimately, the controllability, yaw stability, and safety of the pitch-controlled HAWT led it to narrowly win over the ducted airflow accelerating design. The following figure shows a sample of our decision-making process when choosing our current design.

Table 2: *Analytic Heirarchy Process*

	Cut in speed	Power Stability	Rotor Speed Control	Low Speed Power Performance	Yaw Performance	Braking at High Wind	Vibration	Originality	Manufacturability
Cut in speed	**1**	**1**	**1**	**1/2**	**1/2**	**1/2**	**3**	**3**	**3**
Power Stability	**1**	**1**	**1**	**1/2**	**1/2**	**1/2**	**3**	**3**	**3**
Rotor Speed Control	**1**	**1**	**1**	**1/2**	**1/2**	**1/2**	**3**	**3**	**3**
Low Speed Power Performance	**2**	**2**	**2**	**1**	**1**	**1/2**	**5**	**5**	**5**
Yaw Performance	**2**	**2**	**2**	**1**	**1**	**1**	**5**	**5**	**5**
Braking at High Wind	**2**	**2**	**2**	**2**	**1**	**1**	**5**	**5**	**5**
Vibration	**1/3**	**1/3**	**1/3**	**1/5**	**1/5**	**1/5**	**1**	**1**	**1**
Originality	**1/3**	**1/3**	**1/3**	**1/5**	**1/5**	**1/5**	**1**	**1**	**1**
Manufacturability	**1/3**	**1/3**	**1/3**	**1/5**	**1/5**	**1/5**	**1**	**1**	**1**

3 Aerodynamics

3.1 Rotor Blade Design

Three major parameters for optimization were blade airfoil, blade diameter and tip speed ratio. The team sought a contour with a high lift-to-drag ratio and benign stall characteristics. After surveying several candidate airfoils, the team chose the SG6043 airfoil, as seen in figure 1a and 1b. However, the SG6043 airfoil demonstrated relatively high cut-in speeds. Therefore, our design will use a pitch mechanism to adjust the angle of attack for optimal power generation and minimal cut-in speed. The testing will occur at relatively low Reynolds numbers, which allows us to use a thin airfoil such as the SG6043 without separation.

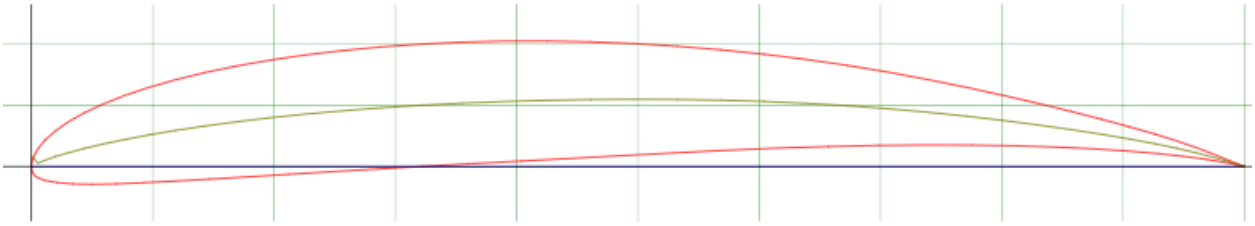

(a)

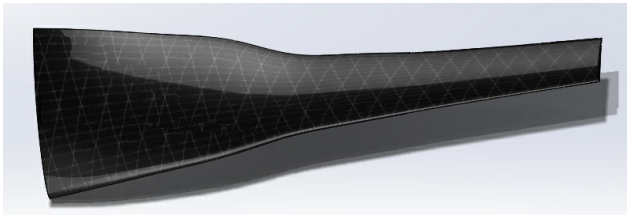

(b)

Figure 1: *(a) SG6043 airfoil; (b) airfoil planform*

Another selection criterion was the tip speed ratio. With the SG6043, the maximum Cl/Cd is about 40 at an angle of attack of 9° at the operating Reynolds number (figure 2). With the Cl/Cd and an operating wind speed of 11 m/s, the tip speed ratio was 3.5, (corresponding to a maximum RPM of 1700). This was deemed to be the optimal rotation speed to obtain a desirable tip speed ratio.

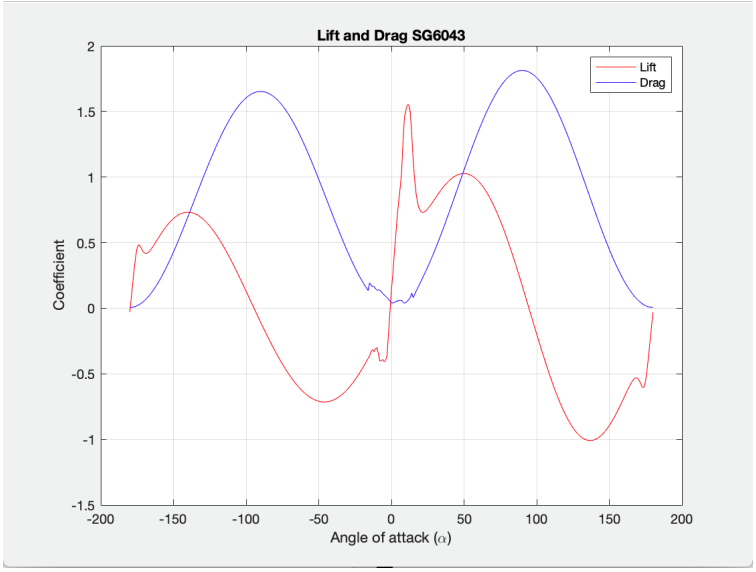

Figure 2: *Cl/Cd versus Angle of Attack for SG6043 Airfoil*

For the optimization of the rotor design a blade element momentum theory (BEMT), including tip loss, and axial and angular induction was used to predict and fine tune the performance of the rotor blades. Using the desired parameters, the blades were initialized using the 'Betz optimum rotor'. An optimization code was then used to modify both chord and twist distribution to achieve the best possible performance and the rotor start speed. The result of this twist distribution optimization code is below in table 3.

Table 3: *Pitch and chord length distribution table*

r/R	r (m)	Chord (m)	Pitch (deg.)
0.1	0.0225	0.06	28.8608
0.2	0.045	0.0568	17.5637
0.3	0.0675	0.0519	11.7628
0.4	0.09	0.0455	7.9538
0.5	0.1125	0.0329	5.5646
0.6	0.135	0.0284	4.1409
0.7	0.1575	0.0246	2.8004
0.8	0.18	0.0222	1.7051
0.9	0.2025	0.0203	0.7947
1	0.225	0.0186	0

Using the BEMT code, several performance curves were generated to predict the performance of the design in the conditions present in Denver. The aerodynamic efficiency and power output of the blades were given by the coefficient of power (C_P) and coefficient of thrust (C_T) versus tip speed ratio (λ) (figure 3).

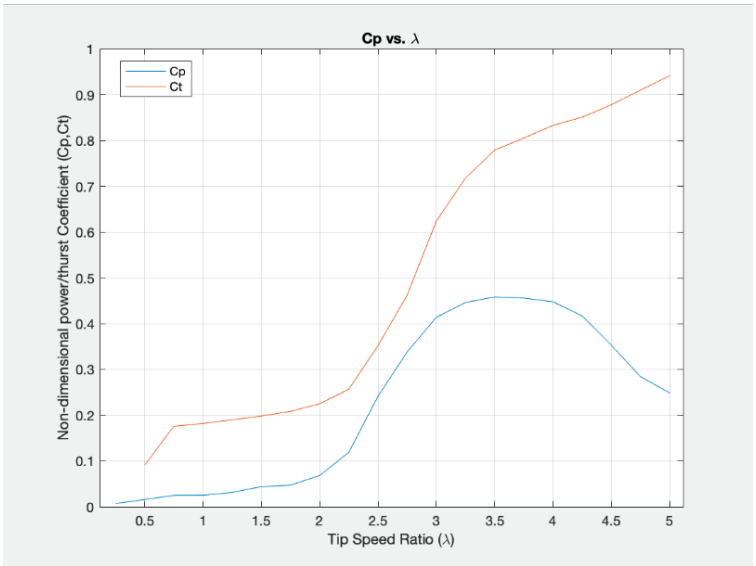

Figure 3: C_P *and* C_T *vs* λ

The theoretical results yielded a maximum coefficient of power to be 0.4586, a reasonable sensible when considering the low Reynolds number and tip speed ratio. Since the air density in Denver is 82% of sea-level density, the cut-in speed was calculated to be 2.8 m/s with a 30° pitch. Furthermore, assuming a peak aerodynamic efficiency, and an 80% overall efficiency the power curve in Denver is shown below in figure 4. The rated power of the turbine is 30.6 W in Denver and 37 W at sea level.

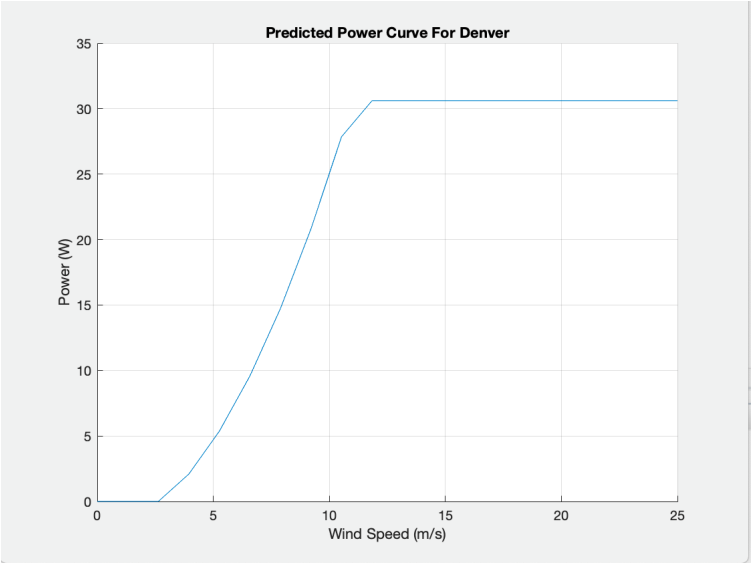

Figure 4: *Predicted Power Curve for Denver*

The maximum possible thrust generated by the rotor was estimated by the following equation:

$$T = \frac{1}{2} C_T \rho U^2 \pi R^2 \tag{1}$$

The value of the coefficient of thrust (corresponding to the value at the design tip speed ratio) was 0.78. Assuming sea level air density, and the maximum competition wind speed of 25 m/s, the highest thrust force that the turbine would sustain was found to be 38.8 N. Under testing conditions at the competition, the pitching mechanism can be used to lower the generated thrust forces at 25 m/s, however an overestimation was used to provide greater strength to the overall structure of the turbine.

3.2 Pitch Mechanism

The turbine will use an SAB Goblin 3 helicopter tail rotor pitch mechanism (figure 5) to regulate turbine pitch. This is connected to an analog servo via a pushrod and universal joint. Pitch angle is regulated via a PWM pulse sent to the pitch servo.

Figure 5: *Collective Pitch Mechanism*

4 Blade Manufacturing

Although the rotor strength test did not result in rotor failure, multiple wind tunnel tests did result in the catastrophic failure of 3D printed blades. As a result, the team opted to fabricate blades from a carbon fibre mold. Team advisors informed the team of the structural integrity of these blades, which they have used for helicopter teams. For this reason, the team was also confident that the manufacturing process, though unique in the history of the UMD Wind Terpines, would be easily and cheaply implemented through our academic and graduate advisors.

5 Generator Selection and Optimization

In the interest of economy and feasibility, the team decided to optimize an off-the-shelf AC motor for use as an electrical generator rather than construct a generator in-house. Retrofitting the components of an existing motor allows us to optimize power output without devoting time and resources to the manufacture of a stator, housing, and other mechanical components. The use of an off-the-shelf motor makes the process of interfacing the generator to the controls set-up significantly less complex as well. The motor we selected, a Turnigy Gimbal Motor 5208, features a three-phase output that can be connected into a rectifier to output DC current as shown in the main circuit schematic (figure 7).

If there were no social restrictions on lab use, our next steps would have helped us optimize our Turnigy Gimbal Motor for our purposes. To do so, we first would find an efficiency value for the turbine with the generator as purchased. The test would be conducted in one of the two wind tunnels available on campus. Next, we would take apart the motor casing, exposing the wire, unwind the wire, and count the number of turns. The number of turns is proportional to the KV, so to alter this value, we would multiply the number of original turns by the factor by which we wished to change the KV. This would determine the new number of turns required for the first step of optimization (figure 6). Finally, this process would be repeated several times until we reached an efficiency that was sufficiently close to optimal.

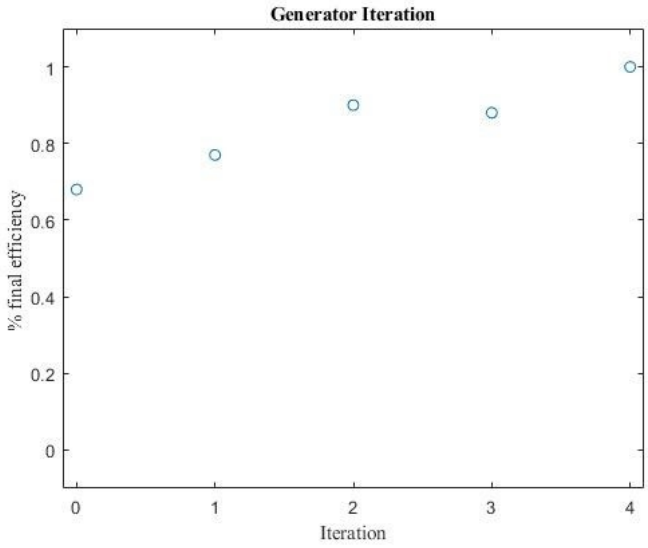

Figure 6: *Modification of KV generator iteration plot*

6 Powering Controllers Sensors, and Actuators

The power for the actuators and sensors is provided by a 5V DC-DC regulator. This regulator is fed by the voltage from the generator. (figure 7) When voltage from the generator drops below 5V, these components will instead draw from the load, which provides 5V DC power regardless of turbine state. This results in negative power during mode 0 operation.

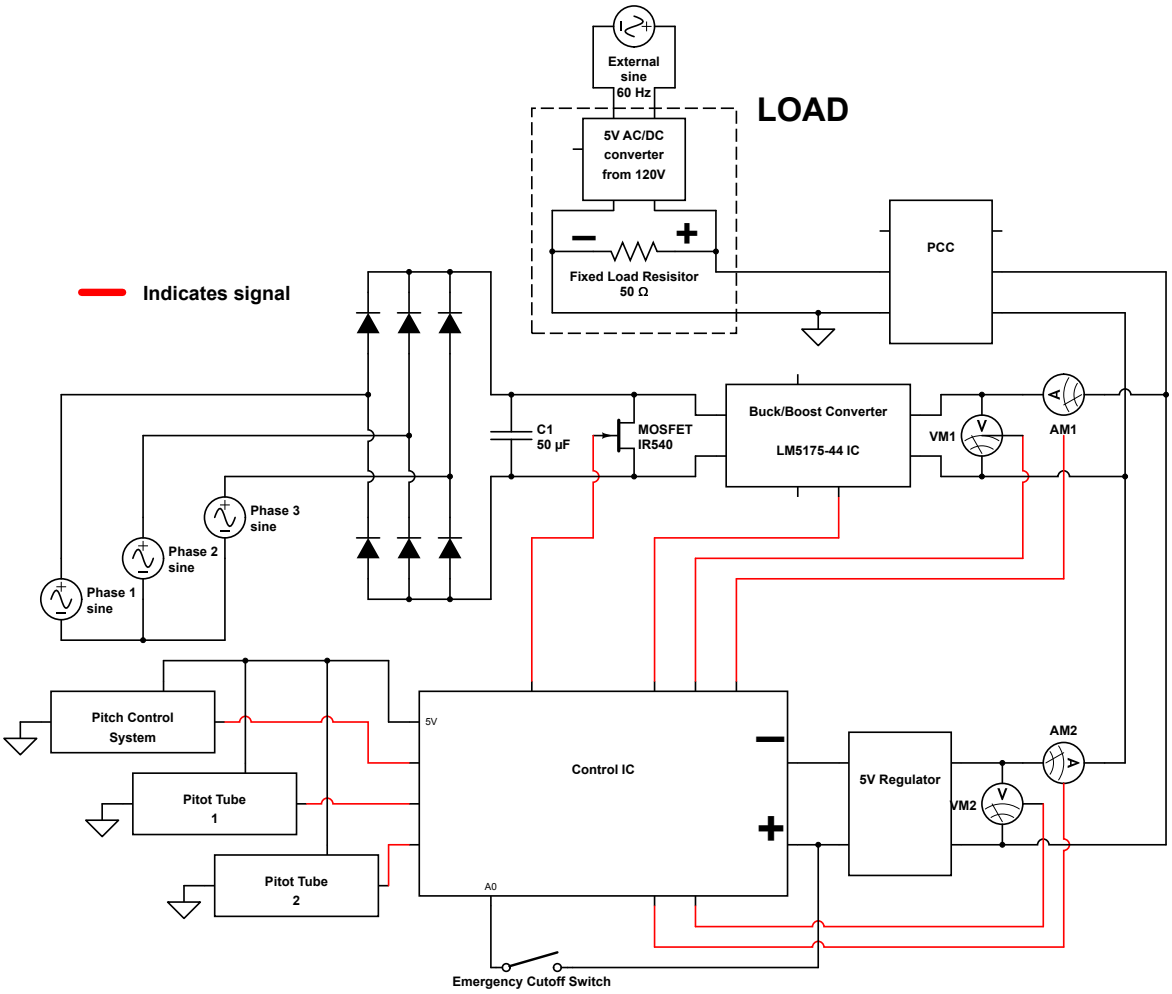

Figure 7: *Control Schematic*

6.1 Power Rectification and Regulation

The generator we have selected provides a three-phase AC output, which is standard for commercial wind power generation. However, the competition mandates a DC power output, necessitating the use of a rectifier. Typical full wave rectifiers consist of diodes which consume more power than the Schottky diode bridge rectifier implemented in our design. This rectifier resolves the three phases as the power is fed into the buck/boost converter, as seen in the circuit diagram (figure 7).

High-fidelity power conversion is necessary for efficient production and use on the load-side and other power consuming sub-systems, such as the buck/boost controller, Arduino, and servos. Noise is inherent in the generation of power by a wind turbine, but it can be mitigated by the implementation of a resistor-capacitor (RC) circuit. The capacitor blocks low-frequency signals

from passing through to output and channels these signals to ground, effectively filtering the noise in the three-phase output.

In order to control generator torque during mode 1 operation, a buck-boost converter is controlled to change the voltage from the generator to a different PCC-side voltage. This voltage, fed to the load resistor, provides optimal rotor torque and electrical power generation. During mode 2, the converter is set to a fixed torque and power setting. The buck-boost converter we selected was the Texas Instruments LM5175, as it is capable of handling voltages up to 60V, well beyond the highest limit of 48 set by the competition.

6.2 Safety Control Mechanism

The turbine will constantly monitor an emergency cutoff switch. The switch will be nominally closed, meaning the Arduino will receive a "high" signal during regular operation. If the switch is pressed, the Arduino receives a "low" signal, indicating little to no voltage-in at the pin. This will trigger a control mechanism that will transition to mode 3 operation, which is emergency shut-down mode. The pin associated with this switch must read "low" for three consecutive readings as a precautionary measure, deterring erroneous readings from shutting down the turbine.

7 Turbine Control

7.1 Description of Overall Control Strategy

The overall control strategy (figure 7) uses pitch control, generator torque control, and electrical braking to achieve a smooth power curve and consistent rated power above rated wind speed. A finite state machine is used to transition between four discrete modes of operation. Although the code for controlling the turbine was not implemented, the overall architecture and controller designs are described.

7.2 Description of Sensors and Actuators

The turbine will be equipped with sensors and employ closed loop feedback control on a series of actuators in order to achieve robust control throughout its operational range. The sensors and actuators used are as follows:

Sensors:

1. 1x Adafruit Reflective IR sensor, detecting shaft rotational speed
2. 1x 30A ACS712 current sensor
3. Voltage sensor V1: measures voltage direct from generator
4. Voltage sensor V2: measures voltage from buck-boost converter
5. 2 Matek ASPD-7002 Pitot-static tube sensors mounted around the outside of the rotor disk

These sensors provide an estimate of wind speed, rotational speed, and power generated by the turbine and are sufficient to perform closed-loop control of turbine power and RPM in modes 1 and 2.

7.2.1 Sensor Fusion

A Kalman filter is employed during mode 1 operation (below rated speed) to ensure a consistent estimate of tip speed ratio and ensure close tracking of optimal Cp. It iteratively updates estimates for tip speed ratio and measurement error using the rotational speed of the shaft, wind speed measurements from the pitot-static tubes, and the measured power of the turbine. The relationship of tip speed ratio, measured power and current estimate of position on the C_p-TSR curve is given by

$$\lambda_{est}^3 = \eta \frac{1}{2} \rho A \Omega^3 R^3 C_P(\hat{\lambda}) P_{el}^{-1} \tag{2}$$

where η is an experimentally determined calibration constant, and a measure of conversion efficiency. This measurement is 'fused' with the pitot-static tube measurements using a live filter to create smooth and accurate estimates of TSR despite yaw error in the pitot tubes and error in rotational speed estimates.

7.2.2 Actuators

- Turbine Pitch servo
- Variable buck/boost converter to control motor reactive torque
- MOSFET power bleed transistor

The pitch position is set directly from a PWM pulse input to the pitch servo. The generator torque will be controlled by varying the voltage of the output to the load in the operating condition with $U_{wind} < U_{rated}$. This changes the effective resistance of the load resistor, while power varies smoothly, according to the relationship:

$$R_{eff} = \frac{V_{buck}^2}{P} \tag{3}$$

where V_{buck} is the voltage experienced by the load resistor from the buck-boost converter and P is the power generated by the turbine. This voltage is controlled using a PWM signal fed into the gate driver circuit that controls the buck-boost converter. These three actuators allow full closed-loop control of power and RPM across all operating modes.

7.2.3 Microprocessor

The Arduino Uno is used for all turbine sensing, actuation and control. This microprocessor was chosen for its ease of use and low power consumption, as well as its many pinouts.

7.3 Dynamic Control

Dynamic control is the lowest level of control, describing how physical inputs and control outputs are related through controllers. As seen in figure 8, four main regions of possible windspeeds exist.

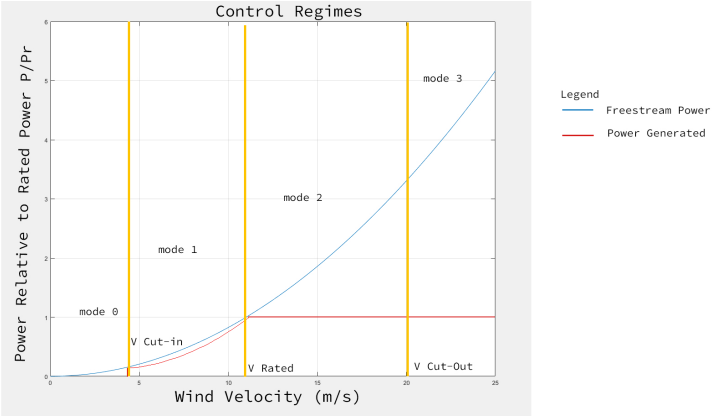

Figure 8: *Illustration of Overall Control Strategy*

7.3.1 Mode 0: Start-up

Mode 0 operation seeks to bring in net positive power as fast as possible. It sets the buck-boost converter to the limit voltage of 45V to decrease effective resistance in the load, minimizing motor torque. The limit of 45V was chosen because it provides a buffer of 3V for fluctuations in buck/boost converter output. The blades are set to the maximum torque angle for the design cut-in speed of 2.5 m/s.

7.3.2 Mode 1: Below Rated Speed Operation

Mode 1 operation seeks to maximize C_p at the given wind speed. This requires control of tip speed ratio (TSR). The pitch system is fixed for maximum power at rated TSR for the duration of mode 1. Motor torque is used to control TSR, controlled via the duty cycle sent to the gate driver circuit. See 'sensor fusion' section for determination of TSR. A PID feedback controller regulating TSR using motor torque (seen below in figure 10) is used for mode 1 operation. The voltage seen at the PCC will vary between 3 and 45 volts to ensure the optimal effective resistance as seen by the generator. At rated speed, 45 volts are needed to maintain steady state RPM.

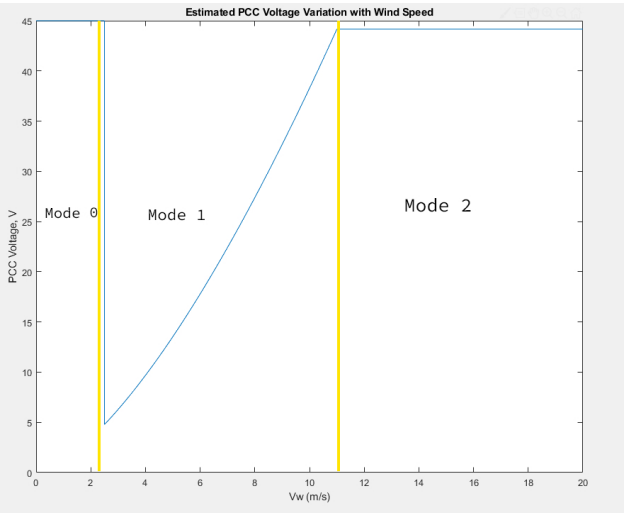

Figure 9: *Illustration of Overall Control Strategy*

Figure 9 shows the predicted voltage values that the buck-boost converter will generate across operating conditions. During mode 1 operation, the voltage is set so that the electrical power generated is equal to the optimal mechanical energy harvested by the rotor disk. During mode 2 operation, voltage is set constant at the value it achieved at rated wind speed.

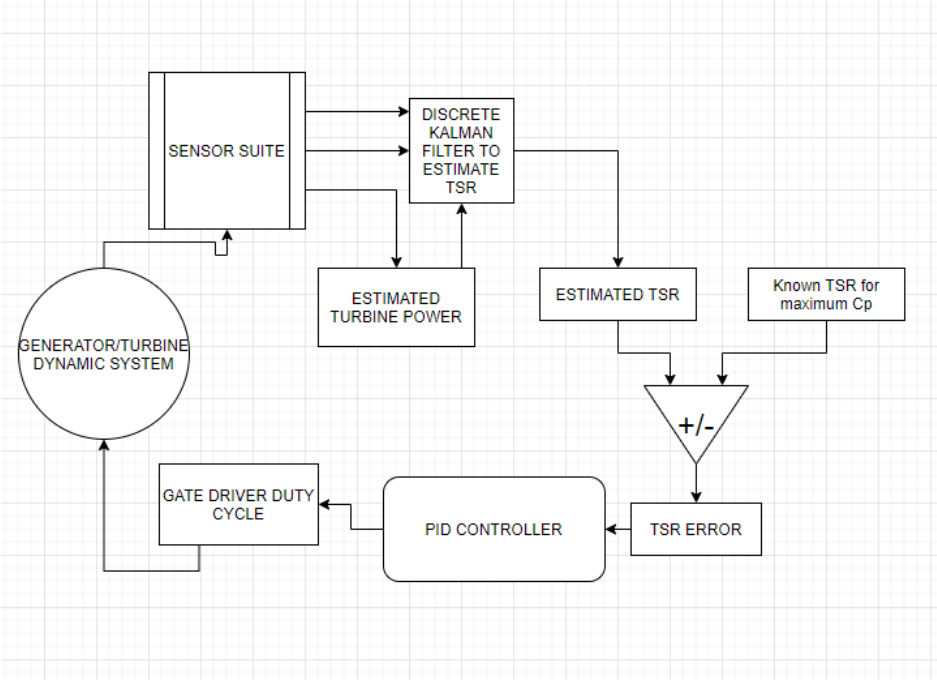

Figure 10: *Mode 1 Control Loop*

7.3.3 Mode 2: Above Rated Speed Control

Mode 2 control, shown in figure 11, performs feedback on the pitch mechanism instead of the generator torque as the primary form of control. It takes advantage of the generator RPM-power relationship, maintaining constant RPM by feathering into the wind. The PWM value sent to the pitch servo is the output of a PID controller that takes in rotor speed as an input. The rotor speed is controlled to be constant at the rated RPM, which was found using the following equation:

$$\Omega_r = \frac{\lambda_{opt} U_r}{R} \tag{4}$$

The motor torque will be nominally set to the torque for rated power generation. This value is found using the following equation, and the corresponding buck-boost duty cycle will be found experimentally. It is roughly the same as the motor torque at the end of mode 1 operation.

$$Q_{ref} = \frac{\rho \pi R^5 C_{p,max}}{2\lambda_{opt}} \Omega^2 \tag{5}$$

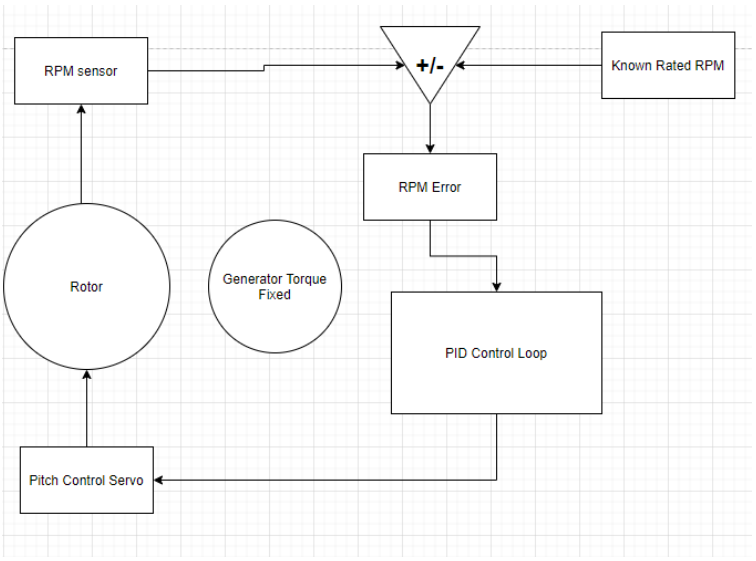

Figure 11: *Mode 1 Control Loop*

7.3.4 Mode 3: Shutdown

Shutdown mode is achieved by feathering the blades beyond the negative angle of attack where aerodynamic torque acts in the opposite direction. The ratcheting bearing in the turbine head keeps the blades from spinning in the opposite direction. Additionally, the MOSFET heat dissipation transistor brake is set high which effectively shorts the generator terminals, causing large damping due to high generator torque. This allows for rapid braking even in high wind conditions. The load will not receive power in this condition due to the power from the generator being dissipated as heat in the MOSFET. We selected the IRF540 Power MOSFET for this application, as its power dissipation capacity exceeds our requirements, and its threshold voltage is compatible with the Arduino control unit. The MOSFET can dissipate up to 150 W, and its threshold voltage sits somewhere between 2 and 4 volts, which is perfect as our Arduino can supply up to 5. The MOSFET's built in heatsink prevents overheating. During this condition, the 5V DC from the load powers the controller, sensors, and actuators, drawing negative power.

7.4 Supervisory Control

Supervisory control describes the control of turbine states, and transitions between dynamic modes. The architecture of the supervisory controller is a discrete finite state machine. This is a form of control logic that monitors inputs and transitions between operating modes as determined by a set of logic conditions. As the turbine senses external inputs, it changes between operating modes by traversing a behavior tree shown in figure 12 and table 4. A sensor process is running during every mode of the finite state machine that monitors all of the critical measurements: airspeed, RPM, turbine power at points 1 and 2, and the emergency shutdown switch.

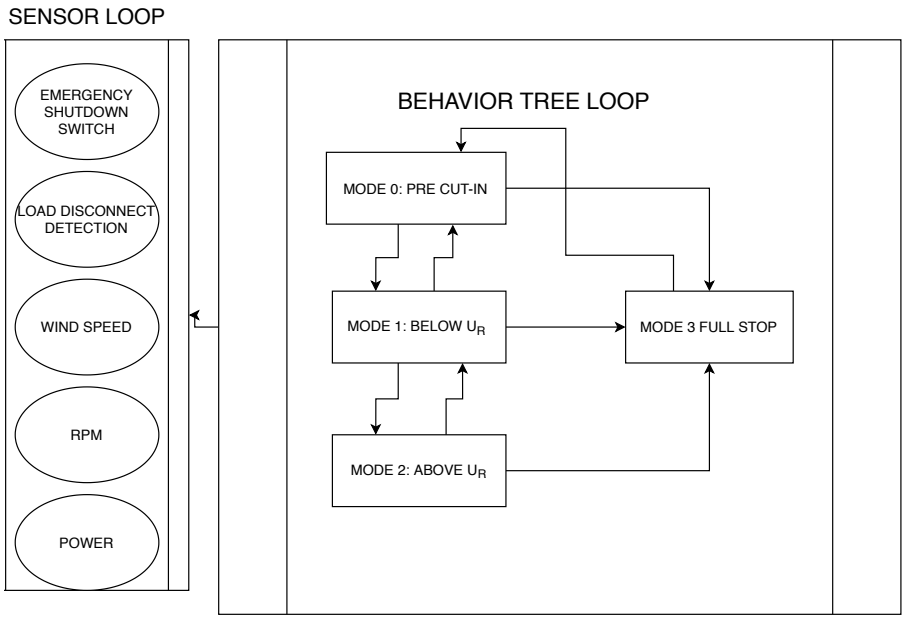

Figure 12: *finite State Machine Diagram*

Table 4: *Finite State Machine Transition Logic. Describes transition from mode [column] to mode [row]. Elements describe cases where condition is satisfied and transition occurs. "X" signifies that case does not occur.*

Full Behavior Tree of Turbine States					
		From			
		0	1	2	3
To	0	X	$P > P_0$ for $t > \varepsilon$	X	Emergency Shutdown OR Load Disconnect OR $P_w > P_{max}$ for $t > \varepsilon$
	1	$P < P_0$ for $t > \varepsilon$	X	$P > Pr$ for $t > \varepsilon$	Emergency Shutdown OR Load Disconnect OR $P_w > P_{max}$ for $t > \varepsilon$
	2	X	$P < P_r$ for $t > \varepsilon$	X	Emergency Shutdown OR Load Disconnect OR $P_w > P_{max}$ for $t > \varepsilon$
	3	Wind speed below cutout for $t > t_{wait}$ AND $RPM < RPM_{rated}$ for $t > t_{wait}$ AND $P < P_{rated}$ for $t > t_{wait}$	X	X	X

7.4.1 Detection of Load Disconnect

Detecting when the load has been disconnected from the turbine is critical to the function of the state machine, as it is one of the conditions for transition to mode 3 operation (turbine shutdown).

In order to detect load disconnect, the sensor loop monitors the difference between power sent to the IC, sensor, and actuator system through the 5V controller and the power through the buck-boost converter. The difference is the power drawn by the load. If this value is zero, the load has been disconnected. A filter is applied to this value to remove noise and if it drops below $P_{crit} = 30W$ for a defined set of time, all states are directed to transition to mode 3 operation.

8 Full Configuration

Overall, the UMD Wind Terpines has developed an adaptation of a traditional 3-blade horizontal-axis wind turbine. Figure 13, below shows the final 3D model of the turbine. Important elements to note are the pitot tube sensors used for wind speed feedback, a pitch mechanism behind the nose cone for added control, and the grid fin for passive yaw.

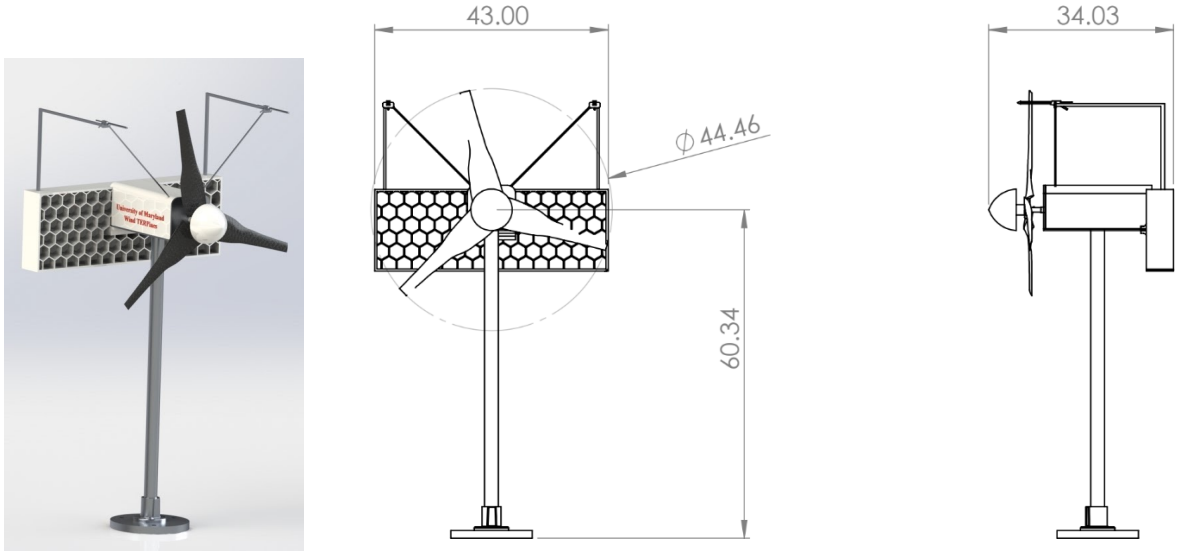

(a) (b)

Figure 13: *(a) 3D render of the tower assembly; (b) 2D render of the tower assembly*

8.1 Tower Design

All tower components were modeled and rendered using Solidworks 2019. Component design focused on meeting structural requirements while simplifying the manufacturing processes and reducing costs. The tower assembly as seen in figure 14 consists of: the baseplate, the tower attachment, the tower, the top plate, and the plate attachment.

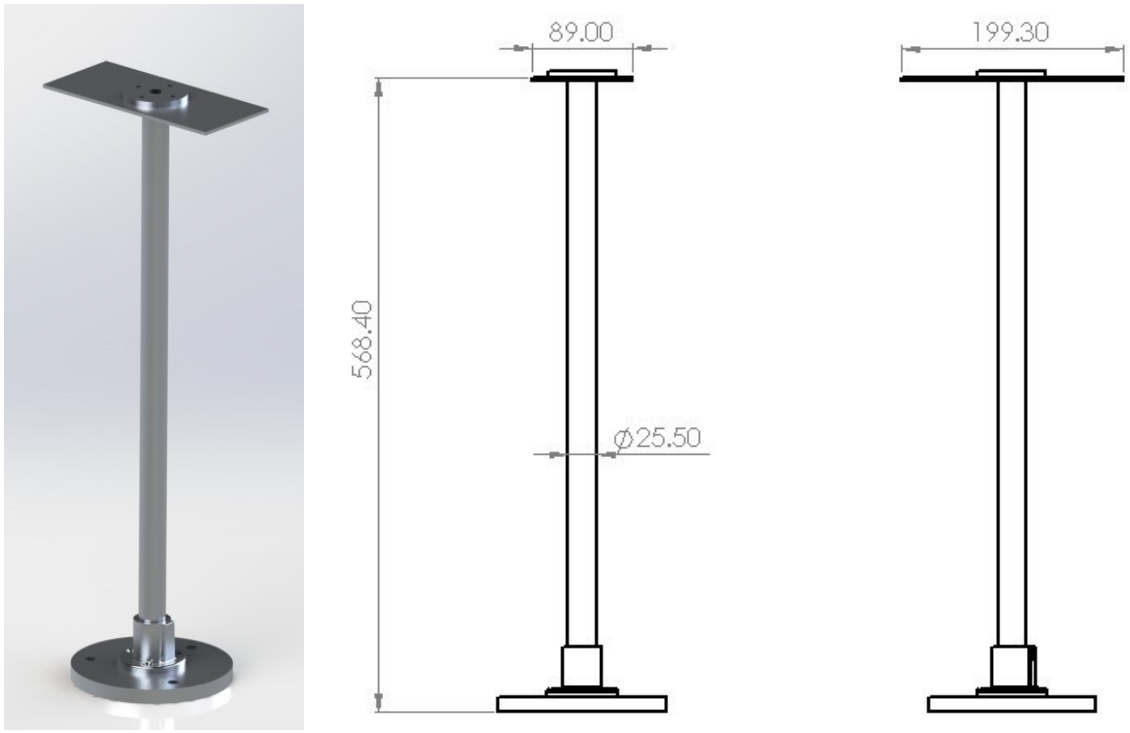

(a) (b)

Figure 14: *(a) 3D render of the tower assembly; (b) 2D render of the tower assembly*

8.2 Yaw System

To save energy and simplify the yaw control of the turbine, the team opted for passive yaw control. A grid fin was selected to properly orient the tower towards the wind while reducing the size of the tail mechanism. The grid fin, shown in figure 15 is connected to the nacelle plate by four bolts. A honeycomb mesh was selected to maintain strength while maximizing the internal surface area. This internal surface area is approximately 0.38 m^2 which is much greater than the recommended amount of 5% of the swept area or 0.008 m^2. The increased area increases the dynamic response of the turbine to a change in wind direction. Ultimately, this reduces yaw vibrations and increases energy capture. The grid fin would have been 3D printed out of PLA to allow for rapid and accurate manufacturing.

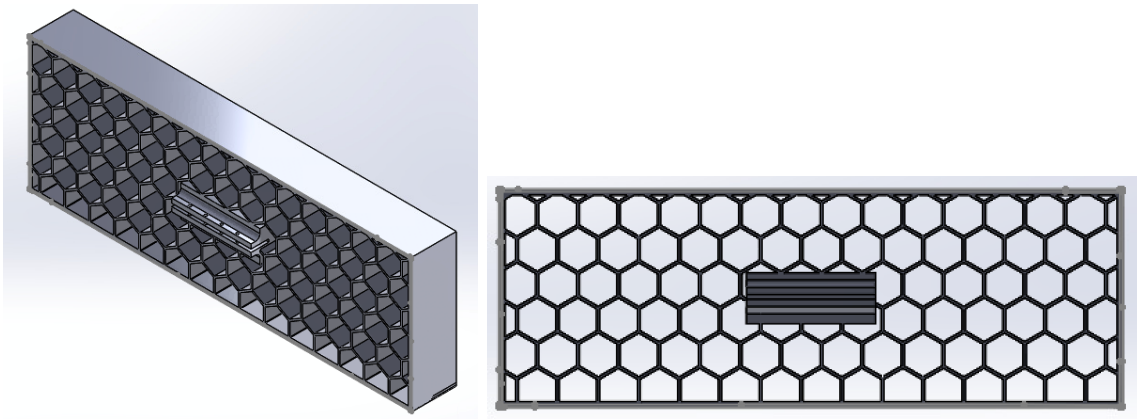

(a) (b)

Figure 15: *(a) Grid fin isometric; (b) Grid fin front view*

9 Looking Back and Looking Ahead

Over the course of this academic year, the Wind Terpines have been thrilled to work on developing a design for a turbine to test in Denver. In the beginning, every decision made was informed in a big way by the process of designing and completing the mid-year checkpoints. First, the dynamometer gave many of our students a foundation for understanding how motors and generators worked, how to begin prototyping for a big project, and how to use and code for basic electronic sensors and actuators. That initial project also helped our team get our feet on the ground in developing an effective team structure. A photo of our original dynamometer is shown below in figure 16.

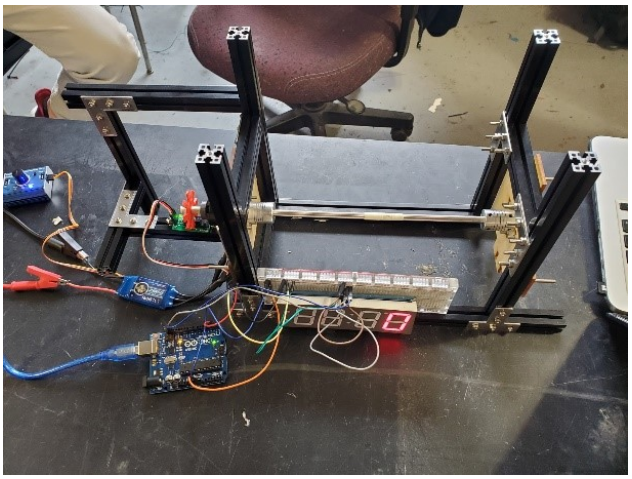

Figure 16: *Photo of the original dynamometer*

When we returned for the spring semester, we found the dynamometer so useful that one of our first tasks was to make a second one so that more than one team could use it for testing at any given time. For example, one group used it for testing modified generators, while the other team was preparing our second milestone for the rotor strength testing. Figure 17 is an image of our rotor test, the last milestone prior to the public health crisis. The test showed us that we could have some confidence in the strength of our rotor, but we have made some alterations since that

day. The primary difference in our rotor for the final design is that the blades are designed to be manufactured using a carbon fiber layering technique used often by the UMD Helicopter team.

Figure 17: *Rotor strength test*

In the end, the University of Maryland closed its doors just weeks after the rotor strength milestone. Since then, the team has relied on the experience we gained during the Fall semester and the start of Spring to further develop our design. We are thankful that the new milestone requirements this year enabled us to gain hands-on experience that we otherwise might have missed because of the pandemic.

If the semester had not been interrupted, we would have loved to do some additional testing and prototyping. In particular, the subteam in charge of the generator was looking forward to testing many iterations of a manually wound generator. Additionally, our team planned to test the thrust strength of the carbon fiber blades by fixing a blade into a cantilevered position and applying a weight to the far end. This configuration would test the thrust forces required to induce failure in the blade. A similar test was planned for the tensile strength test for the blades. Finally, the controls subteam was looking forward to putting each of our control modes to the test in the form of simulations. This would allow us to tune for response rate and optimize the system for a predictable behavior in the Denver testing tunnel.

As a whole, the UMD Wind Terpines are disappointed that we never had the chance to fully prototype and test our turbine. However, we have dedicated significant energy into developing a turbine model that we think had a shot at winning in Denver. Because we will not have the chance to compete in the physical testing this year, we are extremely hopeful that this learning process has provided next year's competition team with a solid foundation for success.

References

Giguère, P. and Selig, M.S., "New Airfoils for Small Horizontal Axis Wind Turbines," ASME Journal of Solar Energy Engineering, Vol. 120, May 1998, pp. 108-114.

J.F. Manwell and J.G. McGowan. *Wind Energy Explained.* Wiley, 2009

“Sizing Your Wind Turbine Tail,” Windy Nation. [Online]. Available: https://www.windynation.com/jzv/inf/wind-turbine-tail-fin-sizing-your-wind-turbine-tail. [Accessed: 27-Mar-2020].